Research Paper

Analysis of Scars and Keloids by Focused Ion Beam/Scanning Electron Microscopy: Distinguishing Between Hypertrophic Scars and Keloids

Running head: Hypertrophic Scars Versus Keloids

Hisashi Migita, MD[*], Hideaki Rikimaru, MD, PhD[*], Yukiko Rikimaru-Nishi, MD[*†], Noriyuki Koga, MD, PhD[*], Koichi Watanabe, MD, PhD[*‡], Keisuke Ohta, PhD[†], Kei-ichiro Nakamura, MD, PhD[†], Kensuke Kiyokawa, MD, PhD[*]

[*]Department of Plastic and Reconstructive Surgery and Maxillofacial Surgery, Kurume University School of Medicine, Kurume, Japan

[†]Division of Microscopic and Developmental Anatomy, Department of Anatomy, Kurume University School of Medicine, Kurume, Japan

[‡]Division of Gross and Clinical Anatomy, Department of Anatomy, Kurume University School of Medicine, Kurume, Japan

Corresponding Author:

Hideaki Rikimaru, MD, PhD

Department of Plastic and Reconstructive Surgery and Maxillofacial Surgery, Kurume University School of Medicine

67 Asahi-machi, Kurume, Fukuoka 830-0011, Japan

Tel: +81-942-31-7569; Fax: +81-942-34-0834

E-mail: Hi_rikimaru@yahoo.co.jp

Conflict of Interest and Source of Funding: The authors have no financial interest to declare in relation to the content of this article. This paper presents the results of a study carried out after the receipt of grants-in-aid for scientific research (JSPS KAKENHI Grant Number: 15K10959). The authors have no financial interest to declare in relation to the content of this article.

ABSTRACT

Background: Histological differentiation between hypertrophic scars (HS) and keloids has been considered difficult. In this study, we analyzed differences in the three-dimensional tissue architecture between HS and keloids using focused ion beam/scanning electron microscopy (FIB/SEM).

Methods: Five specimens each of normal skin, normotrophic scars (NS), HS, and keloids were investigated. Three sites in each specimen were observed by FIB/SEM tomography, resulting in an observation of 15 sites per tissue type. We identified fibroblasts and macrophages, and assessed the contact ratio and the mode of intercellular contact (planar contact or point contact). The significance of differences among the four tissue types was determined by Fisher's exact test.

Results: In normal skin, contact between fibroblasts and macrophages was observed at all 15 sites, and the mode of contact was always planar. There was contact at 87% of the NS sites (planar: point = 80%: 7%). In HS, contact was seen at 80% of the sites (planar: point = 20%: 60%). In keloids, contact was only found at 15% of the sites (planar: point = 7.5%: 7.5%). The intercellular contact ratio showed no significant differences among normal skin, NS, and HS; however, a significant difference was noted between these tissues and keloids. The intercellular contact mode also showed no significant difference between normal skin and NS, but a significant difference between these tissues and HS.

Conclusions: These histopathological findings suggest that FIB/SEM tomography is useful for distinguishing between HS and keloids, and can provide important knowledge for understanding the pathogenesis of keloids.

INTRODUCTION

Wounds heal by scarring, usually by formation of normotrophic scars (NS), although hypertrophic scars (HS) or keloids develop occasionally. There have been various reports on the differences between HS and keloids, both of which involve excessive dermal fibrosis that is related to dysregulation of changes in cellularity during the wound healing process in predisposed individuals. In patients with HS, redness and swelling only affect the boundary of the wound, while pruritus is most severe at three to six months after injury and then resolves spontaneously.[1] On the other hand, keloids tend to spread beyond the boundary of the wound and gradually progress, as well as being associated with moderate to severe pain.[1] While HS have inflammatory characteristics and resolve spontaneously, keloids are refractory and tend to relapse, as well as showing the tumor-like characteristic of invasive proliferation into the surrounding healthy skin. However, a keloid is not actually a tumor and seems to develop due to loss of the mechanism regulating collagen homeostasis.[2,3] Thus, there are clear clinical differences between HS and keloids, but pathological examination by light microscopy or electron microscopy reveals proliferation of collagen fibrils in both lesions,[4] and it is difficult to distinguish between them. Therefore, it is thought that HS and keloids share certain similarities,[4] but the etiology and pathogenesis of keloids have not been clarified and effective treatment has not yet been established.

A focused ion beam/scanning electron microscope (FIB/SEM) combines a focused ion beam with a scanning electron microscope and has been primarily used in the engineering field.[5] Unlike conventional electron microscopes (scanning and transmission electron microscopes), FIB/SEM tomography allows hundreds or even thousands of slices to be observed at a single site by continuous surface milling of a tissue sample with an ion beam. Then data acquired from these numerous slices are used for three-dimensional reconstruction to analyze the fine details of tissue and cellular architecture. In this study, we analyzed the

three-dimensional structure of HS and keloids by FIB/SEM tomography to identify differences between them.

MATERIALS AND METHODS

Patients

This study was conducted according to the principles of the Declaration of Helsinki and its revisions, and was approved by the Institutional Review Board of Kurume University (Study Number 12139).

Twenty patients treated at the Department of Plastic and Reconstructive Surgery and Maxillofacial Surgery of Kurume University Hospital participated in this study and underwent biopsy. Before enrollment, all patients gave written informed consent. A total of 20 biopsy specimens were obtained during standard surgical procedures. These biopsies were divided into five samples each of normal skin, NS, HS, and keloid scars. Clinically, NS were defined as white scars with elevation of less than 2 mm above the normal surrounding skin, while HS were defined as red or pink scars with elevation of more than 2 mm above the normal surrounding skin. This cut-off point was based on the height parameter in the Vancouver Scar Scale,[6] which is commonly used for assessment of burn scars. A keloid was defined as a scar that was elevated and extended beyond the dimensions of the original wound site or lesion. NS were caused by a dog bite on the forearm, funnel chest surgery, auriculoplasty, and traffic accident injury of the thigh, while HS were caused by gynecological surgery, burns to the thigh, traffic accident injury of the thigh, crush injury of the elbow, and auriculoplasty. Keloid scars were caused by auriculoplasty, ear piercing, thyroid surgery, burns to the thigh, and unexplained minor chest injury. The characteristics of the four groups of patients are shown in Table 1.

Harvesting and Processing of Biopsies

Biopsies were harvested after disinfection of the site and local infiltration with a lidocaine solution containing 0.5% epinephrine. Samples for immunohistochemistry were fixed with 4% paraformaldehyde (pH 7.4) in phosphate-buffered saline (PBS) (pH 7.4). Resected specimens were immersed overnight in 30% sucrose in PBS and were subsequently embedded in optimal cutting temperature compound (Sakura Tissue-Tek, Tokyo, Japan) for freezing. Frozen specimens were cut into 5-μm thick sections on a cryostat, and were mounted on glass slides coated with poly-L-lysine. Five sections were made from each biopsy specimen.

Immunohistochemistry and Confocal Laser Scanning Microscopy

The sections were washed three times with PBS and blocked by using a solution containing 1% gelatin and 0.1% Triton X-100 in PBS. Then the sections were incubated overnight at 4°C with rabbit anti-Iba1 antibody[7] (1:5000 dilution; Wako, Osaka, Japan) and mouse anti-HSP47 antibody[8] (1:1000 dilution; clone M16.10A1; Enzo Life Science, Farmingdale, NY, USA). After three washes in PBS (pH 7.4), the sections were reacted for 2 hours at room temperature with a secondary antibody cocktail comprising Alexa488 Fluor-conjugated goat anti-mouse IgG (1:400 dilution, Molecular Probes, Eugene, OR, USA) and Alexa568 Fluor-conjugated goat anti-rabbit IgG (1:400 dilution; Molecular Probes). Nuclei were counterstained with 4'-6-diamino-2-phenylindole (DAPI). Representative sections were observed under a confocal laser scanning microscope (FV-1000; Olympus, Tokyo, Japan). By viewing each section under a 40× objective lens, five fields were randomly selected for analysis. Macrophages and fibroblasts were respectively identified as Iba1-immunoreactive (IR) and HSP47-IR cells in the upper dermis, and cells showing emission from both the nucleus and cytoplasm were counted. For semi-quantitative analysis, the total number of

macrophages and fibroblasts per high-power field (400×) was counted as Iba1-IR and HSP47-IR cells, respectively, using Image J software (National Institutes of Health, Bethesda, MD, USA). Then the mean number of each cell type per high-power field was calculated (Table 2).

FIB/SEM Tomography

Five specimens each of normal skin, NS, HS, and keloid were used for ultrastructural analysis. The superficial dermis was observed in each specimen because it was previously reported as the site of keloid formation.[9] The tissue specimens were trimmed into cubes (5 × 5 × 5 mm) and were pre-fixed using half Karnovsky solution (2.5% glutaraldehyde and 2% paraformaldehyde). Then the specimens were cut into 2 × 2 × 1 mm sections to facilitate staining. After further fixing in the same fixative, post-fixing was done by using a combination of the ferrocyanide-reduced osmium method and the osmium-thiocarbohydrazide-osmium method to enhance membrane contrast.[10] In brief, after three washes in cacodylate buffer, the specimens were post-fixed for 2 hours at 4°C in cacodylate buffer containing 2% osmium tetroxide and 1.5% potassium ferrocyanide. Then the specimens were washed three times with distilled water and immersed in 1% thiocarbohydrazide solution for 1 hour.

After five washes with distilled water, the specimens were further immersed in 2% osmium tetroxide in distilled water. After washing three times with distilled water, the specimens were stained en bloc overnight with 4% uranyl acetate dissolved in a 25% methanol solution for contrast enhancement. After washing with distilled water again, the specimens were dehydrated in an ethanol series (25%, 50%, 70%, 80%, 90%, and twice at 100% for 10 min each), followed by infiltration with epoxy resin (EPON 812, TAAB, Reading, UK) and polymerization for 72 hours at 60°C. The resin blocks were trimmed to 2 ×

5 mm and one surface was exposed by using a diamond knife. This exposed surface (designated as the block surface) was coated with a thin layer of evaporated carbon to prevent charging and backscattered electron imaging was performed by field emission SEM (Quanta 3D FEG, FEI, Eindhoven, the Netherlands). Serial images of the block face were acquired by repeated cycles of surface milling and imaging using Slice & View G2 operating software (FEI).

For reconstruction, the milling pitch of each image was set at 100 nm/cycle and the total size of the reconstruction volume was 80 × 70 × 60 μm (Fig. 1a).[11] Specimen surface milling was performed with a gallium ion beam at 30 kV and a current of 100 pA. SEM image acquisition parameters were as follows: beam current = 46 pA, dwell time =10 μs/pixel, image size = 2048 × 1768 pixels (93.2 × 80.4 μm), and pixel size = 45.5 nm. The image stack thus obtained was analyzed with Avizo 8.0 software (VSG Inc., Bordeaux, France) (Fig. 1b). Using this software, fibroblasts (colored green) were identified as cells with an elongated nucleus that were surrounded by collagen fibrils (Fig. 2a) and macrophages (colored yellow) were identified as cells with numerous finger-like protrusions and many endocytic vesicles (Fig. 2b), while mast cells were colored violet. The three-dimensional structure of these cells and the surrounding tissue was depicted (Fig. 1b). Observation was conducted on 5 specimens of each tissue type (normal skin, NS, HS, and keloid). Three sites in the dermis of each sample were observed by FIB/SEM, and images were reconstructed for a total of 60 sites (3 × 5 × 4).

Transmission Electron Microscopy

Ultrathin sections (70 nm) were prepared from the cross section of the FIB/SEM sample and observed with a transmission electron microscope (Hitachi High-Tech, Tokyo, Japan).

Statistical Analysis

Data on the number of IR cells and the other results of immunohistochemical analysis are presented as the mean ± standard error of the mean and were analyzed by using a linear mixed model method.

Three-dimensional FIB/SEM images of normal skin, NS, HS, and keloid were all analyzed by using AVISO software. We first confirmed whether or not there was contact between fibroblasts and macrophages in the 15 images obtained per tissue type, and then evaluated the mode of contact by classification as follows: “planar contact” (≥ 30% of one side of a cell in contact with the adjacent cell), “point contact” (< 30% of one side of a cell in contact with the adjacent cell), and “no contact” (Table 3). Then differences in the mode of contact between each tissue were examined for significance by using Fisher’s exact test.

RESULTS

Double Immunohistochemical Analysis of Cell Distribution

In the normal skin samples, Iba-1-IR and HSP47-IR signals were frequently seen in close proximity (Fig. 3a), and similar findings were also obtained in NS samples (Fig. 3b) and HS samples (Fig. 3c). However, some Iba-1-IR and HSP47-IR signals were not close together in keloid samples (Fig. 3d). The number of Iba-1-IR signals showed a significant difference between normal skin and keloids (Fig. 3e, $P < 0.1$), but there was no significant difference in the number of HSP 47-IR signals (Fig. 3f). The contact ratio was calculated as the number of macrophages in contact with fibroblasts divided by the total number of macrophages. This ratio demonstrated a statistically significant difference between normal skin and HS samples ($P < 0.01$), as well as between normal skin and keloid samples ($P < 0.01$) (Fig. 3g).

FIB/SEM Tomographic Analysis of Cell Morphology and Cell-to-Cell contact

When the mode of contact between fibroblasts and macrophages was assessed in normal skin samples, contact between these cells was observed at all 15 sites and the contact mode was always “planar contact” (100%). In NS samples, contact was seen at 13 of 15 sites (87%), including 12 sites with planar contact (80%) and one site with point contact (7%), while there was “no contact” at 2 sites (13%). In the HS samples, contact was noted at 12 of 15 sites (80%), including 3 sites (20%) with “planar contact” and 9 sites (60%) with “point contact”, while 3 sites (20%) showed “no contact.” In keloid samples, contact was found at only 2 of 15 sites (15%), including 1 site (7.5%) with “planar contact” and 1 site (7.5%) with “point contact.” On the other hand, there was “no contact” at 13 sites (85%) (Table 3).

The contact ratio between fibroblasts and macrophages showed no significant difference among normal skin, NS, and HS, but a significant difference was noted between these three tissues and keloids ($P < 0.01$) (Fig. 4). In short, fibroblasts and macrophages largely maintained contact with each other in the three tissue types of normal skin, NS, and HS, whereas fibroblasts and macrophages showed scarcely any contact in keloid scars.

When the contact mode (“planar contact” or “point contact”) of fibroblasts and macrophages was investigated in the three tissue types excluding keloids, no significant difference was found between normal skin and NS, but there was a significant difference between normal skin/NS and HS ($P < 0.01$) (Fig. 4). This difference arose because the contact mode in normal skin and NS was basically “planar contact,” while that in HS was largely “point contact.” From these results, fibroblasts and macrophages make “planar contact” with each other in normal skin or NS, which changes to “point contact” in HS. On the other hand, fibroblasts and macrophages make almost no contact with each other in keloids.

DISCUSSION

The present study was performed to analyze differences between HS and keloids at the cellular level. FIB/SEM tomography was employed for three-dimensional analysis of the tissue architecture to reveal the mode of cell-to-cell contact between dermal fibroblasts and macrophages. We found that the contact mode between these cells varied among normal skin, NS, HS and keloids. In normal skin and NS, cell-to-cell contact existed between most fibroblasts and macrophages and the mode was planar contact. In HS, contact was also observed between fibroblasts and macrophages, but the mode was largely point contact. In keloid scars, there was very little contact between fibroblasts and macrophages, unlike the other tissues.

Keloids and HS are difficult to distinguish when observed under a light microscope.[1,12] Fibroblasts are the major type of mesenchymal cell in the dermis and are involved in producing collagen and elastin fibers for the extracellular matrix.[13] While there have been many studies on the kinetics of cultured fibroblasts extracted from various tissues and their production of cytokines/chemokines,[14] and specific biomarkers have been proposed for distinguishing both scar types,[15] there is not yet sufficient information to explain the etiology of keloid formation. Even though the cells constituting both HS and keloids are almost the same,[16] the clinical course and prognosis of these lesions are quite different.[12]

It was reported that tight contact between macrophages and fibroblasts precedes active collagen synthesis and fibrogenesis in granulation tissue,[17] while there was no cell-to-cell contact despite the close proximity of both cell types during the granulation process. However, that study relied on TEM observation, only assessing a single cross section. The results might have been different if the authors had been able to analyze the images showing the entire interaction of macrophages and fibroblasts.

Oka et al. also reported that macrophages and fibroblasts temporarily show loose interaction during the granulation process in a rat burn wound model.[18] Although the

significance of this finding has not been clarified, it was obtained by three-dimensional observation. Regarding the interaction of these two cell types in human skin, there have already been reports of studies based on immunohistochemical analysis,[19] but there have been no previous morphological analyses. Several studies have shown that cell-to-cell interaction between macrophages and fibroblasts is involved in tissue fibrosis in pathological conditions, such as chronic conjunctival fibrosis[20] and hepatic fibrosis.[21] It was also reported that such cell-to-cell interaction causes macrophages to release factors that amplify signal transduction and exacerbate inflammation in myocarditis.[22] The authors of these studies concluded that cell-to-cell interaction was involved in fibrosis by analysis of gene expression and cytokine/chemokine profiles, but there was no morphological analysis of the actual cells and tissues. Macrophages and fibroblasts are multifunctional cells that display complex interactions to mutually modulate their behavior, but their combined interactions and functional effects have not been adequately examined during the process of wound healing.

In the present study, comparison of keloids with HS was performed by three-dimensional FIB/SEM tomography, and we found differences that could possibly be related to the etiology of keloid scars. Fibroblasts and macrophages existed in each of the four tissues we examined, but there were differences in the mode and extent of intercellular contact between the tissues. Particularly in keloids and HS, these differences at the cellular level may be of great significance.

Several limitations should be taken into consideration when interpreting our findings. First, FIB/SEM tomography can only analyze very small samples, and this method cannot be used to completely explain the pathology of keloids and HS. Accordingly, it is necessary to compare the results with analysis at the light microscope level. Light microscopy revealed a statistically significant difference between normal skin and HS or normal skin and keloids with respect to the contact ratio of macrophages with fibroblasts. On the other hand, electron

microscopy also showed a significant difference between normal skin and NS in addition to the above-mentioned findings. It seems important that similar findings were obtained by both methods.

Second, only mature keloids and HS were analyzed in the present study. It is unknown at which stage of the wound healing process normal cell-cell interaction is lost and further investigation is required to assess contact of fibroblasts and macrophages during the maturation process of scars.

Third, other methods are needed to prove that differences in cell-to-cell interaction are actually related to the pathogenesis of keloids and HS. It is necessary to clarify in the future how these changes in cell-cell interactions affect changes in cytokine / chemokine secretion and gene expression. Currently, analyses are underway focusing on several targets, such as specific cell adhesion factors.

Despite these limitations, our findings may provide a new focus in the study of keloids and HS. Our morphological investigation of interactions between fibroblasts and macrophages in keloid and HS tissues revealed that there were significant differences between the two tissues. Based on these morphological findings, we hope to clarify the functional effects of differences in cell-cell interactions between keloid and HS tissues.

Finally, FIB/SEM tomography provided new findings that may lead to elucidation of the pathophysiology of hypertrophic scars and keloids.

ACKNOWLEDGMENTS

The authors thank Mr. Ryuhei Higashi, Mr. Akinobu Togo, and Ms. Satoko Okayama for

their technical assistance. The authors also wish to thank Dr. Tomonoshin Kanazawa, Dr. Hitoshi Obara, and Professor Tatsuyuki Kakuma for their help analyzing the large number of samples.

REFERENCES

1. Verhaegen PD, van Zuijlen PP, Pennings NM, et al. Differences in collagen architecture between keloid, hypertrophic scar, normotrophic scar, and normal skin: An objective histopathological analysis. *Wound Rep Reg.* 2009;7:649–656.
2. Shekhter AB, Serov VV. Inflammation, adaptive regeneration and dysregeneration (intercellular interaction analysis). *Arkh Patol.* 1991;53:7–14. (in Russian)
3. Huang C, Murphy GF, Akaishi S, et al. Keloids and hypertrophic scars: update and future directions. *Plast Reconstr Surg Glob Open.* 2013;1:e25.
4. Rockwell WB, Cohen IK, Ehrlich HP. Keloids and hypertrophic scars: a comprehensive review. *Plast Reconstr Surg.* 1989;84:827–837.
5. Knott G, Marchman H, Wall D, et al. Serial section scanning electron microscopy of adult brain tissue using focused ion beam milling. *J Neurosci.* 2008;28:2959–2964.
6. Baryza MJ, Baryza GA. The Vancouver Scar Scale: an administration tool and its interrater reliability. *J Burn Care Rehabil.* 1995;16:535–538.
7. Ohsawa K, Imai Y, Kanazawa H, et al. Involvement of Iba1 in membrane ruffling and phagocytosis of macrophages/microglia. *J Cell Sci.* 2000;113:3073–3084.
8. Kuroda K, Tajima S. HSP47 is a useful marker for skin fibroblasts in formalin-fixed, paraffin-embedded tissue specimens. *J Cutan Pathol.* 2004;31:241–246.
9. Jiao H, Zhang T, Fan J, et al. The superficial dermis may initiate keloid formation: histological analysis of the keloid dermis at different depths. *Front Physiol.* 2017;8:885.
10. Villinger C, Gregorius H, Kranz C, et al. FIB/SEM tomography with TEM-like resolution for 3D imaging of high-pressure frozen cells. *Histochem Cell Biol.* 2012;138:549–556.
11. Ohta K, Sadayama S, Togo A, et al. Beam deceleration for block-face scanning electron microscopy of embedded biological tissue. *Micron.* 2012;43:612–620.

12. Bran GM, Goessler UR, Hormann K, et al. Keloids: Current concepts of pathogenesis (review). *Int J Mol Med.* 2009;24:283–293.
13. Driskell RR, Lichtenberger BM, Hoste E, et al. Distinct fibroblast lineages determine dermal architecture in skin development and repair. *Nature.* 2013;504:277–281.
14. Lee WJ, Choi IK, Lee JH, et al. A novel three-dimensional model system for keloid study: Organotypic multicellular scar model. *Wound Repair Regen.* 2013;21:155–165.
15. Suarez E, Syed F, Alonso-Rasgado T, et al. Identification of biomarkers involved in differential profiling of hypertrophic and keloid scars versus normal skin. *Arch Dermatol Res.* 2015;307:115–133.
16. Köse O, Waseem A. Keloids and hypertrophic scars: are they two different sides of the same coin? *Dermatol Surg.* 2008;34:336–346.
17. Shekhter AB, Berchenko GN, Nikolaev AV. Macrophage-fibroblast interaction and its possible role in regulating collagen metabolism during wound healing. *Biull Eksp Biol Med.* 1977;83:627–630. (in Russian)
18. Oka T, Ohta K, Kanazawa T, et al. Interaction between macrophages and fibroblasts during wound healing of burn injuries in rats. *Kurume Med J.* 2016;62:59–66.
19. Shaker SA, Ayuob NN, Hajrah NH. Cell talk: a phenomenon observed in the keloid scar by immunohistochemical study. *Appl Immunohistochem Mol Morphol.* 2011;19:153–159.
20. Kechagia JZ, Ezra DG, Burton MJ, et al. Fibroblasts profiling in scarring trachoma identifies IL-6 as a functional component of a fibroblast-macrophage pro-fibrotic and pro-inflammatory feedback loop. *Sci Rep.* 2016;6:28261.
21. Pellicoro A, Ramachandran P, Iredale JP, et al. Liver fibrosis and repair: immune regulation of wound healing in a solid organ. *Nat Rev Immunol.* 2014;14:181–194.

22. Amoah BP, Yang H, Zhang P, et al. Immunopathogenesis of myocarditis: the interplay between cardiac fibroblast cells, dendritic cells, macrophages and CD4+ T cells. *Scand J Immunol.* 2015;82:1–9.

Figure Legends

Fig. 1. Three-dimensional FIB/SEM tomography reconstruction of the dermis in normal skin. (a) Low magnification SEM micrograph showing the entire resin-embedded specimen. Small arrows indicate the reconstructed area. Scale bars = 500 μm. (b) Stack of serial images and three-dimensional rendered views of a macrophage (yellow) and a fibroblast (green). Scale bars = 20 μm. Arrow: three observation area of 70 μm width. Ep: epidermis; D: dermis.

Fig. 2. TEM images of a fibroblast and a macrophage. (a) The fibroblast is an elongated cell with protrusions, and collagen fibrils surround the cell periphery. Scale bar = 2 μm. (b) The macrophages has numerous finger-like protrusions (arrows) on the cell surface and many endocytic vesicles (lysosomes and phagosomes) in the cytoplasm. Scale bar = 5 μm. N: nucleus; CF: collagen fibril.

Fig. 3. Double immunohistochemical staining of four tissues: normal skin, normotrophic scar, hypertrophic scar and keloid tissues. Blue: DAPI (nucleus); green: HSP47 (fibroblasts); Red: Iba1 (macrophage). In each specimen of normal skin, normotrophic scar, hypertrophic scar and keloid tissue, the number of macrophages and fibroblasts in 25 visual fields of each group showed no significant differences. Scale bar = 50 μm. White arrow: intercellular contact. Yellow Arrow: no contact. (a) Normal skin. (b) Normotrophic scar. (c) Hypertrophic scar. (d) Keloid. (e) Box plots showing the number of macrophages in four tissue types. There was a significant difference between normal skin and keloid ($*P < 0.1$). (f) The number of fibroblasts in four tissues types. There were no significant differences among the four tissues. (g) The contact ratio of dermal macrophages and fibroblasts in the four tissue types. The contact ratio of macrophages and fibroblasts showed a significant difference between normal skin and hypertrophic scar ($**P < 0.01$) or normal skin and keloid ($**P < 0.01$).

Fig. 4. FIB/SEM analysis of normal skin, normotrophic scar, hypertrophic scar, and keloid tissue. Yellow: macrophages, green: fibroblasts, violet: mast cells, red: nuclei. Scale bar = 2 μm. (a) Normal skin. (b) Normotrophic scar. (c) Hypertrophic scar. (d) Keloid. Images of cells after three-dimensional reconstruction shown in three directions. There was contact between fibroblasts and macrophages (arrow) in normal skin, normotrophic scar tissue, and hypertrophic scar tissue. However, there was no contact between fibroblasts and macrophages in keloid tissue (triangle). Scale bar = 2 μm. The left side Bar graphs showing the contact rate of dermal macrophages and fibroblasts in each tissue. The contact rate of macrophages and fibroblasts decreased gradually. $^{**}P < 0.01$

The bar graphs on the right show the contact mode ratio of dermal macrophages and fibroblasts in each tissue. Planar contact between macrophages and fibroblasts gradually decreased in normotrophic and hypertrophic scars compared with normal skin. $^{**}P < 0.01$. There was a high no contact rate in keloids.

Author contributions:

Migita H designed the study, and wrote the initial draft of the manuscript. Kiyokawa K, Rikimaru H and Rikimaru-Nishi Y contributed to analysis and interpretation of study course and method, and assisted in the preparation of the manuscript. All other authors have contributed to data and reference collection and interpretation, and critically reviewed the manuscript. All authors approved the final version of the manuscript, and agree to be accountable for all aspects of the work in ensuring that questions related to the accuracy or integrity of any part of the work are appropriately investigated and resolved.

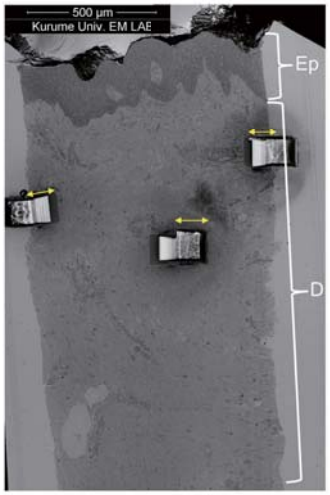

(a)

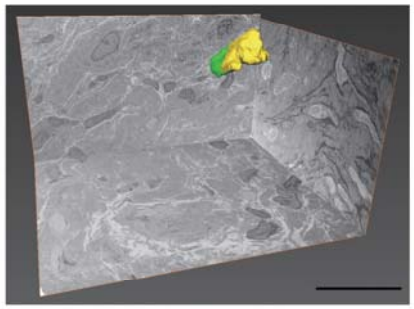

(b)

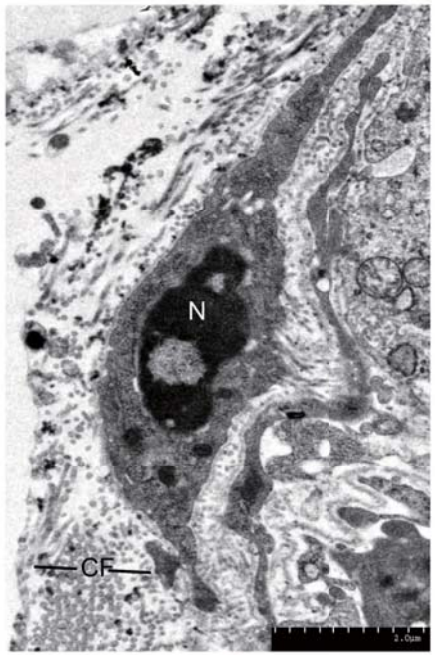

(a)

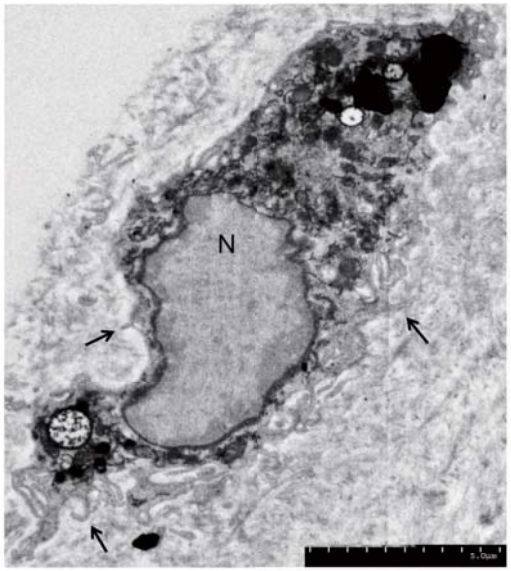

(b)

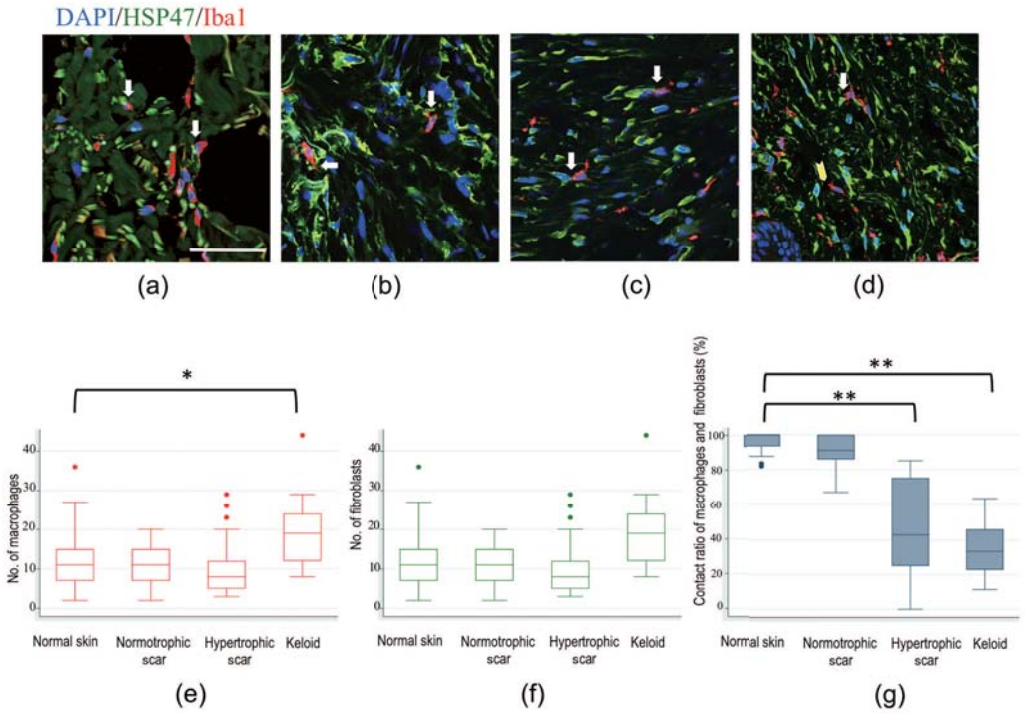
DAPI/HSP47/Iba1
(a)
(b)
(c)
(d)
*
No. of macrophages
0
10
20
30
40
Normal skin
Normotrophic scar
Hypertrophic scar
Keloid
(e)
No. of fibroblasts
0
10
20
30
40
Normal skin
Normotrophic scar
Hypertrophic scar
Keloid
(f)
**
**
Contact ratio of macrophages and fibroblasts (%)
0
20
40
60
80
100
Normal skin
Normotrophic scar
Hypertrophic scar
Keloid
(g)

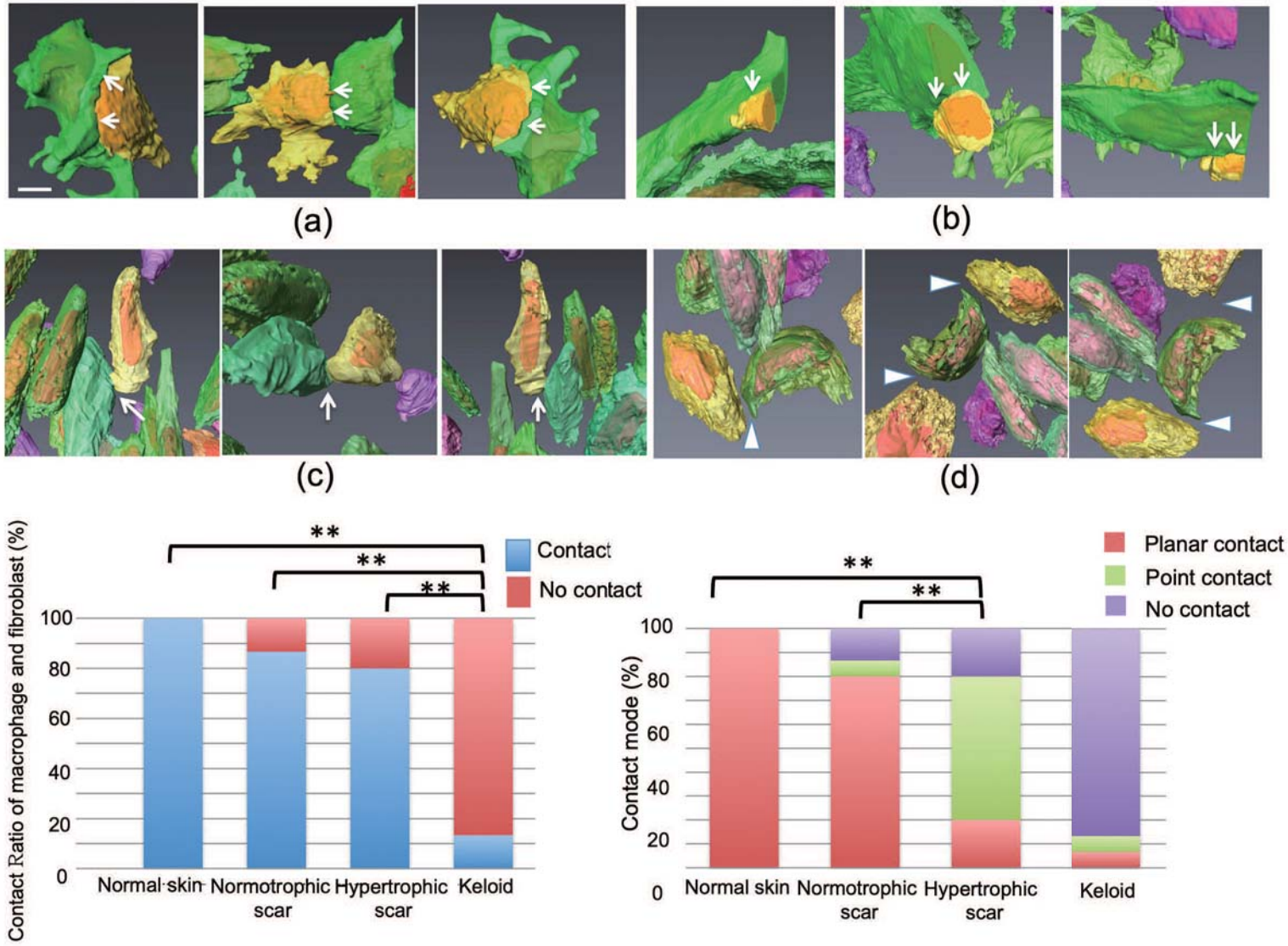
(a)
(b)
(c)
(d)
Contact Ratio of macrophage and fibroblast (%)
100
80
60
40
20
0
**
**
**
Contact
No contact
Normal skin
Normotrophic scar
Hypertrophic scar
Keloid
Contact mode (%)
100
80
60
40
20
0
**
**
Planar contact
Point contact
No contact
Normal skin
Normotrophic scar
Hypertrophic scar
Keloid

Table 1. Characteristics of the Patients

	No. of biopsies	No. of male/female patients	Mean age in years (range)	Mean duration of scar in years (range)
Normal skin	5	3/2	40 (4–78)	—
Normotrophic scars	5	1/4	28.4 (14–54)	3.2 (0.5–8)
Hypertrophic scars	5	1/4	15.6 (4–34)	1.9 (1.25–5)
Keloids	5	1/4	44.6 (11–76)	6.2 (1–15)
Total	20	6/14		

Table 2. Distribution of Dermal Macrophages and Fibroblasts on Double Immunohistochemical Staining

	Normal skin	Normotrophic scars	Hypertrophic scars	Keloids
Total no. of fields observed	25	25	25	25
Total no. of macrophages in 25 fields (range)	307 (2–36)	271 (2–20)	251 (3–29)	481 (8–44)
Mean no. of macrophages per field	12.28	10.84	10.04	19.24
Total no. of fibroblasts in 25 fields (range)	1185 (14–102)	1426 (10–112)	1170 (22–122)	1605 (31–118)
Mean no. of fibroblasts per field	47.4	57.04	46.8	64.2
Contact ratio of macrophages and fibroblasts (%)	95.1	90.0	58.2	33.9

Table 3. Three-Dimensional Evaluation of Intercellular Contact Between Macrophages and Fibroblasts

	Normal skin	Normotrophic scars	Hypertrophic scars	Keloids
Total no. of observations	15	15	15	15
No. of contact sites	15	13	12	2
No. of non-contact sites	0	2	3	13
No. of planar contacts	15	12	3	1
No. of point contacts	0	1	9	1